

Guided Wave Pulse Compression by Airborne Ultrasound Excitation

Kyosuke Shimizu^{1†}, Ayumu Osumi², and Youichi Ito²(¹Grad. of Sci. & Tech., NihonUniv.; ²Coll. of Sci. & Tech., Nihon Univ.)

1. Introduction

We have studied scanning elastic wave source technique using an airborne ultrasound phased array (AUPA)^[1,2], as one of the non-destructive testing methods for concrete structures.

The AUPA of excitation source consists of multiple ultrasound emitters. The ultrasound emitter is premised on driving using mechanical resonance. Therefore, the sound wave is radiated with the time width several times longer than the time width of the input drive signal to the emitter. It is difficult to visualize the boundary between the healthy part and the defective part of the material in the guided wave propagation image which excited by this sound waves, and the defect position cannot be identified effectively.

We have studied aiming at pulse compression of guided waves excited inside concrete using airborne ultrasound modulated by chirp signals, as a method to solve this problem.

In this report, as a basic study, we investigated the effect of pulse compression of the guided wave propagating in a healthy mortar sample by irradiation of airborne ultrasound waves (40k – 60kHz).

2. Pulse compression method

chirp signal is a signal whose frequency changes over time. A linear chirp signal or LFM signal whose frequency changes linearly over time is expressed by the following equation^[3].

$$r(t) = \sin\left\{2\pi\left(f_1 + \frac{f_1 - f_2}{2l_0}t\right)t\right\} \quad (1)$$

where $r(t)$: chirp signal, f_1 : sweep start frequency, f_2 : sweep end frequency, l_0 : sweep time.

The flow for pulse compression of the guided wave excited by the sound wave emitted from AUPA is shown below. First, the above chirp signal (transmitted signal) is input to each ultrasound emitter on the AUPA, and the measurement sample is irradiated with focused sound waves. The guided wave excited in the sample is received by an Acoustic emission (AE) sensor, and a received signal is obtained. Pulse compression can be realized by performing cross-correlation processing of these transmitted and received signals. Cross-correlation processing is expressed by the following equation^[3].

$$c(t) = \int r(t)s(t + \tau)d\tau \quad (2)$$

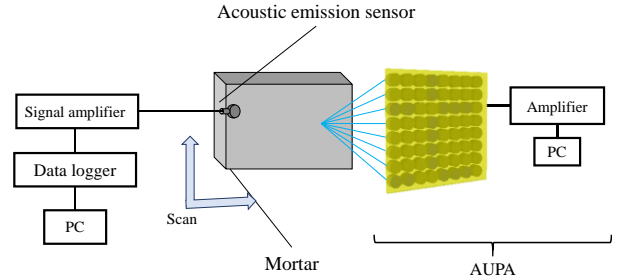


Fig. 1. Schematic of the experimental equipment.

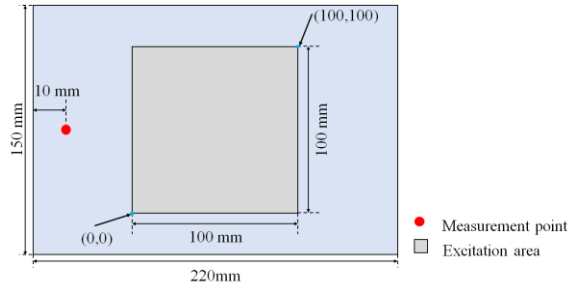


Fig. 2. details of the samples used in the experiment.

where $c(t)$ is the correlation signal, $r(t)$ is the received signal, and $s(t)$ is the transmitted signal.

The pulse width TP after pulse compression is expressed by the following equation^[3].

$$T_P(t) = \frac{1}{f_2 - f_1} \quad (3)$$

3. Measurement method

Figure 1 shows a schematic of the experimental equipment. The equipment was composed of AUPA (resonant frequency 40kHz), function generator (PXIe-6739:NI), amplifier for amplification (self-made, NJM5532D), data logger (USB-6356:NI), AE sensor ((PICO:PAC), preamplifier (2/4/6C: MISTRAS), and a PC that controls peripheral equipment. The AUPA uses an 8×8 (64 mm \times 64 mm) grid array consisting of ultrasound emitters (T4008A1: Nippon Ceramic) with a diameter of 8 mm. The chirp signal used as the input signal to AUPA was $f_1 = 40$ kHz, $f_2 = 60$ kHz, and $l_0 = 2$ ms.

Figure 2 shows the details of the samples used in the experiment. It was made of mortar (25% water-cement ratio) and has dimensions of 220 mm \times 150 mm \times 60 mm. As shown in Fig. 1, it was

arranged corresponding to the focal position of the sound wave at a position of 100 mm from AUPA.

The experiment was performed according to the following procedure. First, high-intensity point-focused sound waves from AUPA were applied to each position of the excitation region shown in Fig. 2 at intervals of 2 mm to generate guided waves in the sample.

These vibration informations were acquired by the AE sensor placed at the measurement position shown in Fig. 2. By performing pulse compression processing on the acquired vibration time waveform, pulse-compressed vibration waveforms corresponding to each excitation position in the measurement area were obtained.

The sampling frequency during waveform recording was 2 MHz.

For comparison, we also verified the guided wave propagation waveform excited by the sound wave irradiation from the AUPA driven by the burst wave with the irradiation cycle number of 10 cycles.

4. Results

First, **Figure 3** shows a guided wave propagation image when driven by 10-cycle burst waves. The result is normalized over the entire measurement range and measurement time. **Figure 4** shows the time waveform at coordinates (0, 50). From Fig. 3, we can confirm the propagation of the guided waves. Also, from Fig. 4, it can be confirmed that the guided wave is generated for about 300 μ s, which is a long time.

Next, **Fig. 5** shows a guided wave propagation image after pulse compression. **Figure 6** shows the time waveform at coordinates (0, 50). The results are normalized in the same way as above. From the results, a sharp rise of the wavefront compared to Fig. 3 can be confirmed. In addition, the pulse of the guided wave shown in Fig. 6 has been shortened from about 300 μ s to about 50 μ s, and the effect of pulse compression can be confirmed.

5. Conclusion

Aiming at realization of pulse compression of guided wave by airborne ultrasonic excitation, excitation of guided wave to mortar sample by chirped wave emitted from AUPA and pulse compression processing of guided wave propagating in the sample were verified. As a result, we confirm the effect of applying pulse compression processing to guided wave.

In the future, we aim to apply pulse compression to mortar samples with defects.

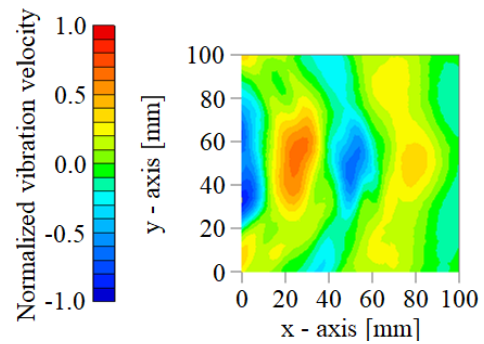


Fig. 3. Guided wave propagation image (10-cycle burst waves).

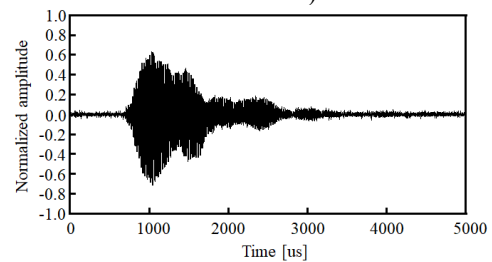


Fig. 4. Time waveform at coordinates (0, 50) (10-cycle burst waves).

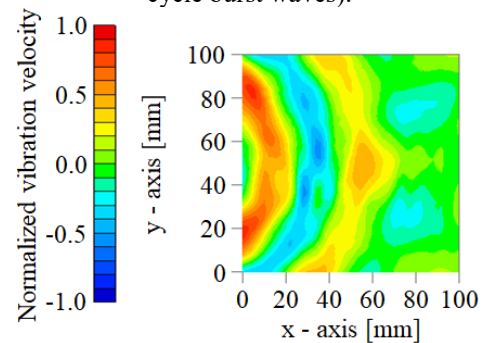


Fig. 5. Guided wave propagation image (after pulse compression).

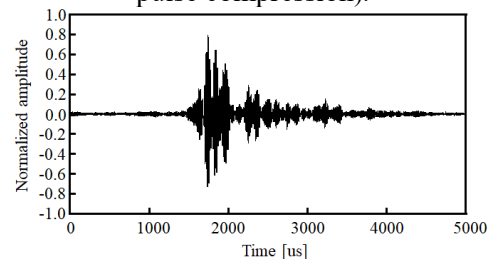


Fig. 6. Time waveform at coordinates (0, 50) (after pulse compression).

Acknowledgment

This work was partly supported by JSPS KAKENHI Grant number 22K04624.

References

1. K. Shimizu, A. Osumi and Y. Ito: Jpn. J. Appl. Phys. 59 (2020) SKKD15.
2. K. Shimizu, A. Osumi and Y. Ito: Jpn. J. Appl. Phys. 61 (2022) SG1050.
3. J.R. Klauder, et. al., The theory and design of chirp radars, Bell Syst. Tech. J. 39, 745 - 808 (1960).